Int. J. Therm. Sci. (2001) 40, 571–580

S1290-0729(01)01245-5/FLA

On the influence of tribo-induced superheating on protective layer formation in dry sliding of metallic pairs

Hisham A. Abdel-Aal

Department of Mechanical Engineering Technology, York Technical College, P.O. Box 54821, Charlotte, NC 28299, USA

(Received 17 December 1999, accepted 8 September 2000)

Abstract — This paper studies the effects of the heat diffusion ability of a rubbing material on wear resistance at high temperatures. These effects are studied with a special focus on the dilution of thermal energy in sliding. The results suggest a correlation between wear transition and the change in the heat transfer limit of a rubbing material. The nature of change in the thermal properties before and after the transition influences the thermal environment within the contacting layers. This controls the kinetics of oxide formation and thereby controls wear. Thermal dilution is a super position of three functions which represent the competing effects of the room temperature thermal properties and their respective variation with temperature. Hence, the change in the thermal properties bears on dilution. The possible relation between thermal dilution and protective oxide formation is studied by examining fretting wear data for two alloys: a Ni-based alloy and a Co-based alloy. Results indicate a strong correlation between the formation of protective oxides and the change in the dilution of thermal energy of the examined alloys with temperature. Moreover, examination of the wear data suggests that a critical ratio between the effects of the conductivity and those of the diffusivity has to be established for favorable wear resistance. This ratio reflects on the intrinsic ability of the material to sustain an oxidative reaction of a controlled rate in which protective glaze oxide layers are formed in a rate that is approximately equal to the rate of oxide layer break down. Therefore, continuous compensation for the removed oxide layer (self-repairing oxides) is established in such a case. © 2001 Éditions scientifiques et médicales Elsevier SAS

high temperature wear resistance / thermal properties / thermal dilution / friction heat / sliding temperature

Nomenclature

A_a	area of conduction	m^2
A_r	real area of contact between the sliding solids	m^2
B_0	thermal effusivity	$W{\cdot}m^{-2}{\cdot}K^{-1}{\cdot}s^{1/2}$
p	average contact pressure	$N{\cdot}m^{-2}$
Q_{diss}	rate of total heat diffusion away from the surface	W
Q_{gen}	rate of total heat generation at the surface	W
U_{slid}	sliding speed	$m{\cdot}s^{-1}$
Z_p	diffusion length	m
$Z_{p_{max}}$	depth from the surface at which a temperature rise 1 % of that at the surface is felt	m
k_0	reference thermal conductivity	$W{\cdot}m^{-1}{\cdot}K^{-1}$
q_a	rate of instantaneous heat diffusion by an individual pair of contacting asperities	W
q_{res}	amount of residual heat	W
r_a	radius of the contact spot between two contacting asperities	m
t_c	duration of a single contact cycle	s

Greek symbols

α	thermal diffusivity of the material	$m^2{\cdot}s^{-1}$
β	temperature coefficient of the thermal conductivity	K^{-1}
η_a	efficiency of an asperity pair to dissipate heat	K
θ_b	bulk temperature rise	K
θ_s	instantaneous temperature rise at the center of contact spot between two asperities	K
θ_{max}	maximum potential temperature rise at the end of the contact cycle	K
θ_m	melting temperature	K
θ_Z	temperature rise at a depth Z from the surface	K
μ	nominal coefficient of friction	
σ_y	yield strength of the material	MPa

Acronyms

HDC	heat diffusion capacity
RRH	ratio of residual heat

E-mail address: haabdela@excite.com (H.A. Abdel-Aal).

MAL mechanically affected layer (equivalent to heat transfer limit)

1. INTRODUCTION

Frictional heat generation at the interface between a rubbing pair may induce gross structural changes within each of the rubbing materials. Such changes may include thermochemical transformations, absorption of gases, depending upon the temperature attained, and protective oxide-layer formation, all of which are related to the wear resistance of rubbing materials operating at high temperatures. It is, therefore, possible that frictional heating can play an important role in enhancing (or degrading) the elevated temperature wear resistance of surfaces. The possible detrimental effects of friction induced heat on wear has recently become a focus of several investigations, the results of which imply a strong correlation between frictional heat accumulation within the mechanically affected layer, MAL, and the transition in wear (mild-to-severe, severe-to-mild, etc.).

Bian et al. [1] recognized that the thermal induced change in a sliding system is an important factor that determines the tribological integrity of a rubbing material. Hence, these authors attempted to link scuffing to frictional heat input. They deduced that the contact temperature is the primary factor that determines the mechanism and rate of wear. Frictional heat (termed also as frictional power) input to the rubbing pair was the basis for several scuffing models which were reviewed by Dayson [2]. Meng [3] suggested that for every sliding system there is a critical frictional-power input. If the operation conditions are such that the frictional power input to the system is less than the critical limit, scuffing (or tribo-failure in general) may be avoided, whereas if that input exceeds the critical limit thermal tribo-failure most likely will take place. The ideas of Meng were modified by Jeng [4] who considered that scuffing is the consequence of the disorientation and the desorption of the protective films formed during sliding due to the intensity of frictional heat input exceeding a critical limit. Thus, according to these models, frictional-heat input, in itself, is not the cause of the failure. Rather, it is the efficiency of heat removal from the interface to the bulk of the material that may be catastrophic. That is, if frictional heat removal is in balance with frictional heat generation thermal failure may be avoided and vice versa.

The idea that tribo-failure is related to the efficiency of heat removal is not new to tribo-analysis. For example, Blok [5, 6], with no experimental evidence, used this idea as a basis for his proposal concerning the constancy of scoring temperatures. Many investigators echoed the same idea in their work. Others have supplied experimental evidence supporting the connection between the accumulation of frictional heat within the MAL and wear regime transition. Wang [7] performed abrasion experiments on hardened 35 Mn2 steel specimens on a dry sand rubber wheel tester at a variety of loads and speeds. The author considered the appearance of tongues on the worn tracks as evidence of frictional heat accumulation on the steel specimen surface. Due to heat accumulation, the hardness decreased and wear regime transition, from soft-abrasive to hard-abrasive, took place. Singh and Alpas [8] observed that the surface temperature of a wrought aluminum alloy (6061AL) worn against an SAE 52100 steel counter face reached a constant value of 395 ± 10 K at the onset of mild-to-severe wear transition. This observation was equally valid for both velocity induced and load induced transitions. Therefore, Singh and Alpas suggested that attainment of a critical temperature is a necessary condition for wear transition. Further evidence supporting this preposition were provided by Zhang and Alpas [9] who studied the wear transition of the same material configuration used in [8] both in dry sliding conditions and under the effect of forced cooling. When the aluminum sample was slid for 500 m at a test load of 98 N and a speed of 0.8 $m \cdot s^{-1}$ without cooling the critical temperature was exceeded and a mild-to-severe wear transition was observed. However, when the aluminum samples were worn under the same load and speed, but were subjected to forced cooling (by circulating chilled water around the sample holder), the critical temperature was not reached, and no transition was observed. Interestingly, moreover, Wilson and Alpas [10] noted that the critical temperature measured in [8, 9] corresponded to the average temperature of a layer of material about 10–100 μm below the nominal contact surface. This depth correlated well with the scale of material that was subjected to deformation and plastic damage during wear (i.e., the MAL). The authors also calculated the flash and the bulk temperatures for the loads and speeds used in their experiments using the method suggested by Lim and Ashby [11]. They found that at all loads and speeds, near the transition, the theoretically calculated bulk and flash temperature contours merged into each other. This implied a drop in the heat transfer limit of the material within the mechanically affected layer. The findings reported in [10] support an earlier postulate made by Buckley [12] who performed several experiments to investigate the dry sliding of copper and bronze specimens. Based on his measurements, Buckley postulated that during sliding, the heat transfer ability of the contacting lay-

ers (interface and substrate) is affected by the surface temperature rise. So that, after a period of continuous sliding, heat will accumulate within the contacting layers, hence leading to both the bulk and the flash temperatures becoming equal. The work reported in [1–11], among others, implies that for each material there is an intrinsic heat transfer (diffusion) limit. When the frictional heat input to the sliding pair exceeds the heat transfer limit of the material failure is likely to occur and vice versa. As such, the criterion for thermally-dominated tribo-failure may be expressed in terms of an equilibrium between the heat generated by friction and the intrinsic heat transfer limit of the sliding pair. That is the ability of the sliding material to diffuse the friction induced thermal load.

The conjecture that an equilibrium between frictional heat generation and the heat transfer limit of a wearing material is a necessary condition for high temperature wear resistance was examined by Abdel-Aal [13, 14]. It was found that the balance between heat generation and heat diffusion by a rubbing pair is, in essence, an equilibrium between the influence of the diffusivity and that of the conductivity (and their respective variation with temperature) on frictional heat transfer. Moreover, it was established [13] that the equilibrium between the effects of the thermal properties is strongly correlated to the self repairing properties of the protective oxide layers formed during sliding. That is the intrinsic ability of the material to sustain an oxidative reaction of a controlled rate in which protective glaze oxide layers are formed in a rate that continuously compensates for the amount of oxide depleted by friction. The equilibrium between thermal property effects bears on the dilution of the frictional heat due to thermal diffusion within the contacting layers of the material. Dilution is also a measure of the intensity (concentration) of heat within the contact area and its immediate vicinity. For the purpose of this work the term thermal dilution is taken to indicate the variation of heat intensity (amount of super heating) within the contact area.

The heat contained within a certain volume of the material is a function of temperature. Wear resistance of the material (or more precisely, wear regime transition [14]) is a function of a critical temperature rise being reached. As such, it is logical to conjecture a connection between an associated critical heat intensity (or alternatively, thermal dilatation) and the wear resistance at elevated temperatures. This connection, in essence, may explain the mechanistic influence of heat intensity on providing a suitable thermal environment that aids the growth of protective oxide layers.

This paper investigates the role of the thermal transport properties on thermal dilution within the mechanically affected layer of a rubbing material, and the effect of this dilution on protective oxide formation during rubbing. The first part of the paper examines the individual role of each of the thermal properties, and their respective variation, on thermal dilution, whereas the second part examines the conjecture that thermal dilution is related to protective layer formation. This is achieved by examining fretting wear data of two alloys: a nickel-based alloy (Ni-20Cr-2Al) and a cobalt-based alloy (Haynes-188) in light of a thermal dilution–temperature curve.

2. THE AMOUNT OF HEAT DISSIPATED BY A SINGLE ASPERITY

The amount of heat flowing away from the contact spot into a solid during the time interval (t_1, t_2) is given by [15]

$$q_{t_1-t_2} = \int_{t_1}^{t_2} \left[\int_A k \frac{\partial \theta}{\partial \eta}(\boldsymbol{r}, t)\, \mathrm{d}A \right] \mathrm{d}t \tag{1}$$

Heat flow within the contacting layers is predominantly one-dimensional. As such, equation (1) may be written, for a nominally flat contact spot in the (X, Y) plane, in the familiar form

$$q_{\mathrm{a}} = -k \frac{\partial \theta}{\partial Z}\bigg|_{Z=0} A \tag{2}$$

In a sliding solid, the maximum temperature is reached at the nominal contact surface. This implies that the thermal properties of the material at the surface, depending on the temperature difference between the surface and the bulk, will be different. To incorporate the effect of the temperature-induced variation in the thermal properties on the surface temperature, the so-called Kirchhoff transformation is applied. As detailed elsewhere [16], this transformation acts as a correction to the constant property solution of the heat equation. Thus, if the constant conductivity surface temperature is given by [4]

$$U_{\mathrm{s}}(t) = \frac{2q_{\mathrm{gen}}}{k_0} \left[\frac{\alpha t}{\pi} \right]^{1/2} \tag{3}$$

then the variable thermal conductivity solution will be given as [15]

$$\theta_{\mathrm{s}}(Z, t) = \frac{1}{\beta} \left[\left\{ 1 + 2\beta U_{\mathrm{s}}(Z, t) \right\}^{1/2} - 1 \right] \tag{4}$$

Differentiating equation (4) with respect to the depth Z we may write

$$\frac{\partial\theta}{\partial Z}(Z,t)=\frac{\partial U}{\partial Z}(Z,t)\bigg|_{Z=0}\left\{1+2\beta U(Z,t)\right\}^{-1/2} \quad (5)$$

Substituting from equation (4) into equation (5), the relation between the variable and the constant conductivity temperature gradient assumes the form

$$\frac{\partial U}{\partial Z}(Z,t)=\frac{\partial\theta}{\partial Z}(Z,t)\bigg|_{Z=0}\left\{1+\beta\theta(Z,t)\right\}^{-1/2} \quad (6)$$

Finally, upon substituting equation (6) into equation (2) the temperature dependent amount of heat penetrating to the contacting layer of the rubbing solid takes the form

$$q_{\mathrm{a}}(\theta)=K_0\left\{1+\beta\theta(Z,t)\right\}\frac{\partial\theta}{\partial Z}(Z,t)\bigg|_{Z=0} \quad (7)$$

Equation (7) may be rewritten, for one-dimensional heat conduction, as [18]

$$q_{\mathrm{a}}(\theta)=\gamma k_0\{1+\beta\theta\}\left[\frac{\theta_{\mathrm{s}}-\theta_{\mathrm{b}}}{Z_{p_{\max}}}\right] \quad (8)$$

where γ is a constant approximately equal to 3.57. Now, if the bulk temperature θ_p is defined as the temperature rise of the solid taking place at the boundary of the thermal layer (which is practically equal to the initial temperature) then $\theta_{\mathrm{b}}\approx\theta(Z_p)\approx 0$. Thus, for practical purposes we may write

$$q_{\mathrm{a}}(\theta)=\{1+\beta\theta\}\left[\frac{\theta_{\mathrm{s}}}{Z_{p_{\max}}}\right]\gamma \quad (9)$$

Equation (9) represents the amount of heat that penetrates through the contact spot into the rubbing material. The equation accommodates the variation in the thermal conductivity of the material with temperature through the incorporation of the temperature coefficient β. As it may be noticed, the sign of the β coefficient affects the amount of heat transferred to the bulk of the material. If the conductivity drops with temperature, the amount of heat penetrating through the material will decrease with temperature elevation. This situation highlights the role of the mating material. That is, if the conductivity of the mating material drops with temperature as well, then it is likely that the generated heat will not be completely dissipated into both materials and heat will accumulate within the contacting layers. Here, if the conductivity of the mating material increases with temperature, the mating material may share a higher thermal load. Hence, depending on the ability of the mating material to dissipate heat, thermal accumulation may be avoided (or regulated). It has to be noted, however, that heat accumulation is not necessarily destructive. Rather, heat accumulation can raise the amount of heat contained within the contact spots. This heat may create a suitable ambient environment that helps interfacial gases to surpass the energy barriers necessary for sustaining an oxidative reaction. In this sense, heat accumulation may promote the formation of a protective oxide layer. Naturally, there are limitations to the benefits of heat accumulation. Moreover, there are intrinsic constraints to the increase of heat content. These are imposed by the change in the thermal properties with temperature and the impact of that change on the ratio between the conductivity and the diffusivity (ρC_p). In that respect, it is beneficial to recall the fundamental definitions of the subject thermal transport properties, these being: the conductivity is the property responsible for transmitting heat from a source to the immediate vicinity of the contact spot; and the diffusivity may be considered as the speed by which the transmitted heat diffuses through a particular area. As such, to maintain the intensity level necessary for protective layer formation, it is necessary for the conductivity to overcome the diffusivity effects at all temperatures. That is, fundamentally, thermal dilution should be at a minimum at all temperatures.

3. THE PENETRATION DEPTH OF A TEMPERATURE STEP

To estimate the thickness of the thermal layer, Z_p, consider that the material and its surface are at some given initial temperature, θ_0. At time t_0^+ the surface is set to a temperature θ_{s}. Now, define a normalized temperature $\overline{\theta}$ that represents the ratio of the temperature rise at a depth Z, to the surface temperature. The temperature field in the material expressed in the new parameter may be written as

$$\frac{\partial\overline{\theta}}{\partial t}=\alpha\frac{\partial^2\overline{\theta}}{\partial Z^2} \quad (10)$$

with the boundary conditions

$$\begin{aligned}&\overline{\theta}=0, \quad t<0, \quad 0<Z<\infty\\ &\overline{\theta}=1, \quad t>0, \quad Z=0\end{aligned} \quad (11)$$

The solution to this problem is [15]

$$\overline{\theta}=\frac{2}{\sqrt{\pi}}\int_{\xi}^{\infty}\exp\left\{-\xi^2\right\}\mathrm{d}\xi=\mathrm{erfc}(\xi) \quad (12)$$

where

$$\xi = \frac{Z}{2\sqrt{\alpha t}} \tag{13}$$

Equation (12) represents the response of the material to a surface temperature step originating at the surface, where the maximum response corresponds to $\overline{\theta} = 1$, while no response is $\overline{\theta} = 0$, i.e., $0 < \overline{\theta}_p < 1$. The equation

$$\overline{\theta}_p = \frac{2}{\sqrt{\pi}} \int_{\xi}^{\infty} \exp\{-\xi^2\}\, \mathrm{d}\xi = \mathrm{erfc}(\xi_p) \tag{14}$$

has the solution ξ_p, unique to a particular $\overline{\theta}_p$. Hence, the maximum penetration depth may be written (after using $\mathrm{erfc}(2) \approx 0.0047$) as

$$Z_{p_{\max}} = Z_{0.01} \simeq 4\sqrt{\alpha t} \tag{15}$$

Substituting from equation (15) into equation (7), and assuming a linear variation in the diffusivity with temperature of the form $\alpha(\theta) = \alpha_0(1 + \delta\theta)$, the amount of heat dissipated through the surface of true contact may be written as

$$\begin{aligned} \frac{q_{\mathrm{diss}}}{A_{\mathrm{c}}} &= -\frac{k_0}{4\sqrt{\alpha_0}} \frac{(1+\beta\theta_{\mathrm{s}})\theta_{\mathrm{s}}\gamma}{[(1+\delta\theta_{\mathrm{s}})t_{\mathrm{c}}]^{1/2}} \\ &= -\frac{B_0\gamma(1+\beta\theta_{\mathrm{s}})\theta_{\mathrm{s}}}{4[(1+\delta\theta_{\mathrm{s}})t_{\mathrm{c}}]^{1/2}} \end{aligned} \tag{16}$$

Plotting equation (16) as $q_{\mathrm{diss}}/A_{\mathrm{c}}$ versus temperature θ_{s} results in a curve that represents the variation in the HDC with temperature. As pointed out elsewhere [18], the maximum HDC may not necessarily be equal to the amount of heat generated at the surface. To investigate the influence of the transport properties, the change in the slope of the HDC is evaluated, this is written as [19]

$$\frac{1}{A_{\mathrm{c}}} \frac{\partial q_{\mathrm{diss}}}{\partial \theta_{\mathrm{s}}} = F_1 + F_2\theta_{\mathrm{s}} + F_3\theta_{\mathrm{s}}^2 \tag{17}$$

where

$$F_1 = \frac{\gamma B_0}{\sqrt{t}} \frac{1 + 2\beta\theta_{\mathrm{s}}}{[1+\delta\theta_{\mathrm{s}}]^{3/2}} \tag{18-a}$$

$$F_2 = \frac{\gamma B_0}{2\sqrt{t}} \frac{\delta}{[1+\delta\theta_{\mathrm{s}}]^{3/2}} \tag{18-b}$$

$$F_3 = \frac{3\gamma B_0}{2\sqrt{t}} \frac{\beta\delta}{[1+\delta\theta_{\mathrm{s}}]^{3/2}} \tag{18-c}$$

The preceding analysis may be extended to accommodate the presence of an oxide film on the contact surface by replacing the thermal conductivity by an *effective* thermal conductivity given by [11] as

$$k_{\mathrm{eq}} = k_{\mathrm{m}}\left[1 + \frac{\zeta}{l_{\mathrm{f}}}\left(\frac{k_{\mathrm{m}}}{k_{\mathrm{ox}}} - 1\right)\right]^{-1} \tag{19}$$

where ζ is the thickness of the oxide layer, l_{f} is the diffusion length in the metal, and the subscripts m and ox denote the thermal conductivity of the metal and the oxide, respectively. Note that k_{eq} inversely varies with the thickness of the oxide layer.

Equations (16)–(18) incorporate an explicit dependence on the thermal effusivity B_0. In particular, each of the quantities q_{diss} and the dilution vary in direct proportion to the value of the effusivity. This indicates that, all parameters being equal, a material that possesses a high thermal effusivity will be able to diffuse a higher thermal load than a material of a lower effusivity. Moreover, from equations (17) and (18), a high thermal effusivity may impose a high thermal dilution. This is not desirable as higher dilution indicates a wide variation in the ability of the material to diffuse thermal loads per unit surface temperature rise. Naturally, the quantities B_0, β and δ are intrinsic to the particular material. As such, balancing the effect of any of these parameters on heat diffusion, or thermal dilution, is fairly constrained by physical limits. However, it is envisioned that careful selection of mating materials based on thermal compatibility criteria may aid in this respect.

The functions F_1, F_2 and F_3 represent the different components of heat dilution. Thus, thermal dilution, according to equations (18-a), (18-b) and (18-c), has three components. The first, represented by F_1, is due to the variation in the thermal conductivity of the material with temperature. The second, expressed as F_2, is due to the variation in the thermal diffusivity with temperature, while the third component, the function F_3, represents a non-linear contribution due to the interaction of the diffusivity and the conductivity coefficients. It is noted that the dilution is a strong function of the temperature coefficients β and δ. Therefore, the errors involved in their evaluation will directly contribute to any uncertainty entrained in the theoretical calculation of heat dilution. Hence, the examination of the influence of the method used in evaluating the temperature coefficients is in order.

In general, the errors involved in estimating β and δ using linear regression for monotonic materials (i.e., materials for which the thermal properties display a single behavior for the entire temperature range $0 < \theta < \theta_{\mathrm{m}}$) is in the order $\pm 0.5\,\%$ [20]. However, when the metal (or alloy) exhibits a local maximum or minimum, infliction

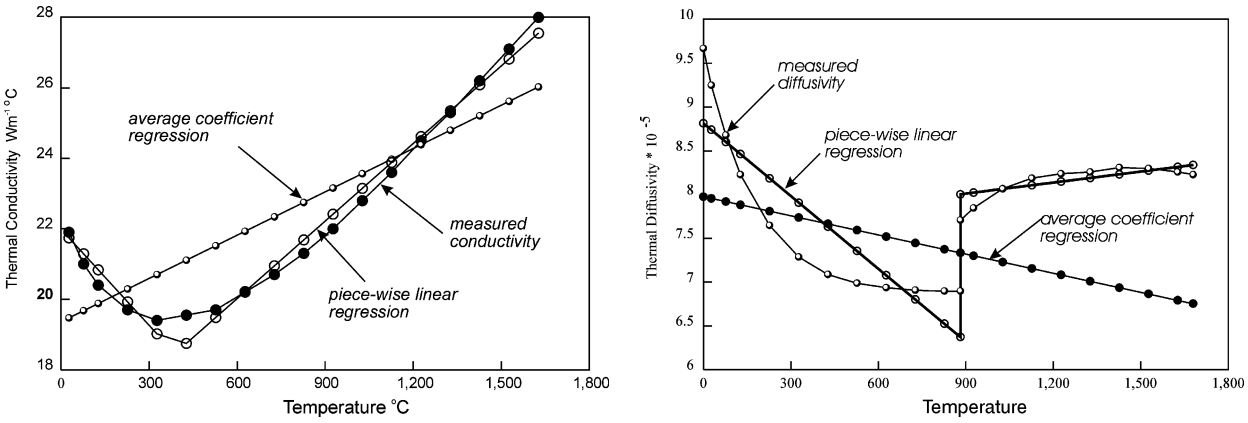

Figure 1. The effect of the regression method on the accuracy of the temperature coefficients of commercially pure titanium. (a) Variation in the thermal conductivity with temperature. (b) Variation in the thermal diffusivity with temperature.

TABLE I
Temperature coefficients for the thermal properties of commercially pure titanium.

Thermal diffusivity, $m^2 \cdot s^{-1}$			Thermal conductivity, $W \cdot m^{-1} \cdot K^{-1}$		
	Coefficient	Temp. range, °C		Coefficient	Temp. range, °C
δ_{ave}	$-1.14 \cdot 10^{-5}$	$0 < \theta < 1627$	β_{ave}	0.000212	$0 < \theta < 1627$
δ_1	−0.000314	$0 < \theta < 882$	β_1	−0.000413	$0 < \theta < 442$
δ_2	$5.478 \cdot 10^{-5}$	$882 < \theta < 1627$	β_2	0.0004697	$442 < \theta < 1627$

point (e.g., titanium and zinc), linear regression using the entire temperature range may result in considerable errors. To minimize the errors involved, the conductivity (or diffusivity) versus temperature plot is treated as a piecewise linear function. Thus, the respective temperature coefficients are determined for each segment of the curve. This procedure is illustrated in *figures 1(a)* and *(b)*, which depict the variation in the thermal conductivity and diffusivity of commercially pure titanium with temperature. It will be noticed that the thermal conductivity exhibits a local minimum value around 440 °C. Similarly, the diffusivity exhibits a local minimum around 880 °C, a temperature which is associated with a phase change from a hexagonally packed α-structure to a BCC structure. For each property, two curves were fitted. The first (denoted average coefficient regression) was calculated assuming that the entire property–temperature curve may be represented by a single line. This line is based on an average temperature coefficient (β average for the conductivity and δ average for diffusivity). The second fit (denoted as 2 linear segment regression) is calculated by assuming piecewise linear behavior. Thus, for each linear segment, a corresponding temperature coefficient was evaluated. The values of those coefficients and the associated temperature range are summarized in *table I*.

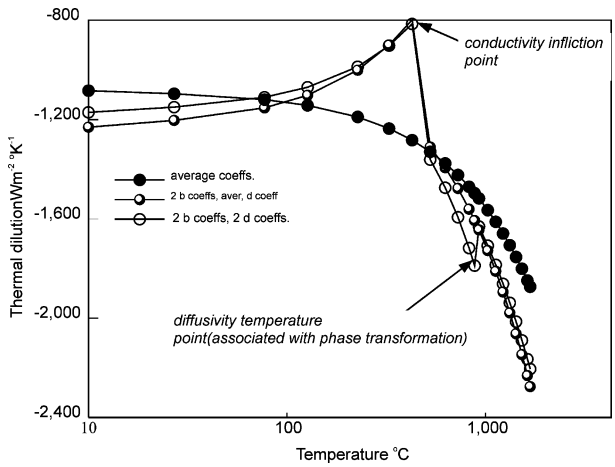

Figure 2. Effect of the temperature coefficients on the calculation of the thermal dilution for commercially pure titanium.

The effect of using the temperature coefficients on calculating the dilution for titanium is shown in *figure 2*.

Thermal dilution was calculated using different combinations of the temperature coefficients. It is noticed that using the piecewise linear coefficients results in a dilution curve that closely represents the physical behavior of the material, that is, a curve which exhibits kinks at temperatures that are in close proximity to the original infliction temperatures for the conductivity and diffusivity, respectively.

4. RESULTS AND DISCUSSION

To examine the proposed connection between the thermal properties and wear transition, two alloys were studied: a nickel-based alloy (Ni-20Cr-2Al) and a cobalt-based alloy (Haynes-188). Each alloy was tested for fretting wear against like material by Bill [21, 22]. Test conditions were as follows: frequency of 80.0 Hz, peak-to-peak amplitude $75{\cdot}10^{-6}$ m and a nominal applied load of 1.47 N. Physical properties of the alloys are summarized in *table II* [23], while *table III* provides a summary of the wear volumes and the coefficients of friction at different test temperatures.

For each of the examined alloys the three functions F_1, F_2 and F_3 were calculated. These are shown in *figure 3(a)* (for the Ni-based alloy) and *figure 3(b)* (for the Co-based alloy). The plots represent the normalized values of the respective functions. The normalization is carried out by dividing the value of each function, at the particular temperature, by the value of the respective function at room temperature. It is noted that for both alloys the dominant function is F_1 which represents the relative effects of the conductivity variation on thermal dilatation. As such, for the purpose of this work only the normalized values of the function F_1 will be correlated to wear data.

The analysis starts by calculating the difference between the heat transfer limit (HDC) of the material and the generated heat q_{gen}. This quantity, termed the residual heat q_{res}, is then used to construct a ratio of residual heat (RRH) $q_{\text{res}}/q_{\text{gen}}$ versus temperature plot. The heat generated at the interface is calculated from [24]

$$q_{\text{gen}}(\theta) = 2.7\mu\sigma_{\text{y}}(\theta)UA_{\text{r}} \tag{20}$$

where $\sigma_{\text{y}}(\theta)$ is the temperature dependent yield strength in MPa. This is calculated by interpolation between the room temperature value and the value at the melting temperature ($\sigma_{\text{y}} = 0$). Hence, $\sigma_{\text{y}}(\theta) = \sigma_{\text{y}}^{\circ}(1 - \theta/\theta_{\text{m}})$. The RRH plot is then inspected for points where it is equal to zero (implying that the HDC is equal to the generated heat), or alternatively, where a change in the slope takes place. The temperatures associated with each point for the particular alloy are subsequently correlated to the transition temperatures extracted from the literature. Thermal aspects of the transition in wear are then examined by analyzing the trends of RRH, the thermal effusivity and the function F_1 before and after the calculated transition temperatures.

Figure 4 depicts the variation in the RRH (solid lines, left scale) and the function F_1 (dashed lines, right scale) with temperature. The curves labeled I and II were calculated using the value of the coefficient of friction at room temperature (see *table III*) and at the respective temperatures. The RRH values corresponding to the temperature at which the friction coefficient changes are plotted as discrete values. Curves III are schematics sketched to indicate the anticipated behavior

TABLE II
Thermophysical properties of the studied alloys.

Alloy	$e{\cdot}10^{-3}$, W·m^{-1}·s$^{-1/2}$	k_0, W·m^{-1}·K	$\alpha_0{\cdot}10^{6}$, m^2·s^{-1}	β, K^{-1}	δ, K^{-1}	T_{m}, K	σ_{y}, MPa
Haynes-188	6.182	10.4	2.83	0.00161	0.00075	1 374	640
Ni-20Cr-2AL	5.744	11.3	3.87	0.00157	0.00037	1 400	570

TABLE III
Experimental fretting wear scar volumes and coefficients of friction [21, 22].

Material		Temperature, °C						
		23	216	327	450	540	650	816
Haynes-188	W, mm$\cdot10^{-5}$	31	7	3	2	7		2
	COF	0.1				0.3		0.4
Ni-20Cr-2AL	W, mm$\cdot10^{-5}$	100		28	19	13	23	1 500
	COF	0.1		0.15		0.2	0.3	0.4

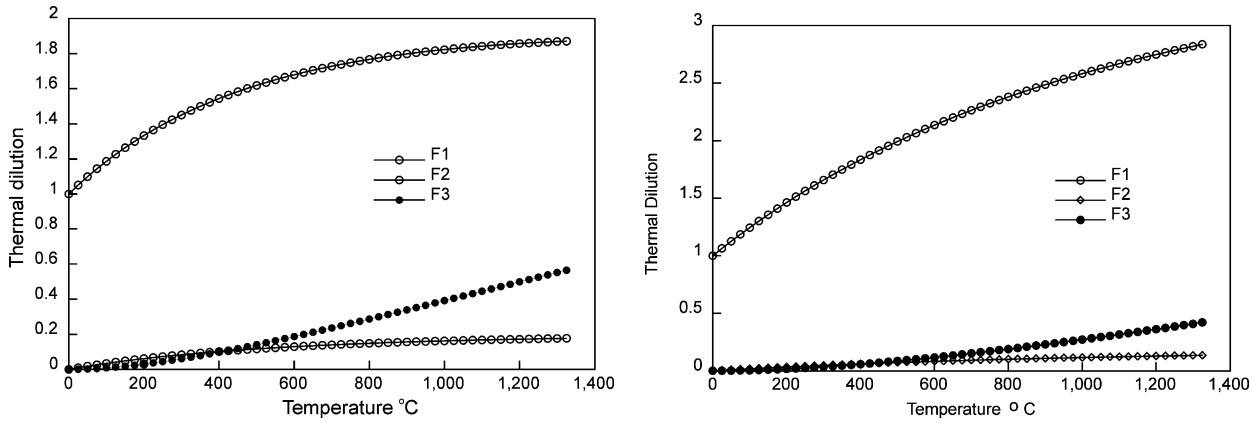

Figure 3. Variation in the components of thermal dilatation (functions F_1, F_2 and F_3) with temperature. The plotted values are normalized by the room temperature values of the respective functions. (a) Variation of the functions for Ni-based alloy Ni-20Cr-2AL. (b) Variation of the functions for Co-based alloy Haynes-188.

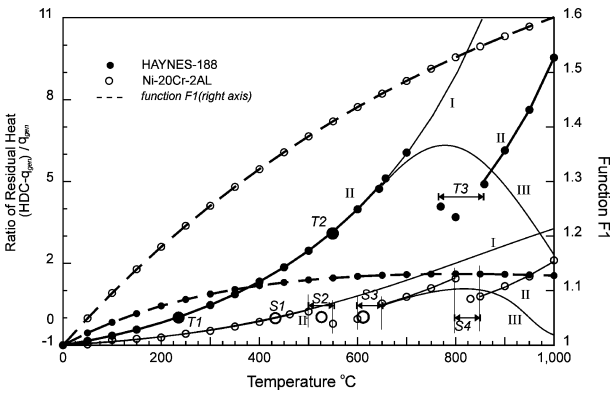

Figure 4. The variation in the ratio of residual heat RRH (solid lines, left scale) and the function F_1 (dashed lines, right scale) with temperature.

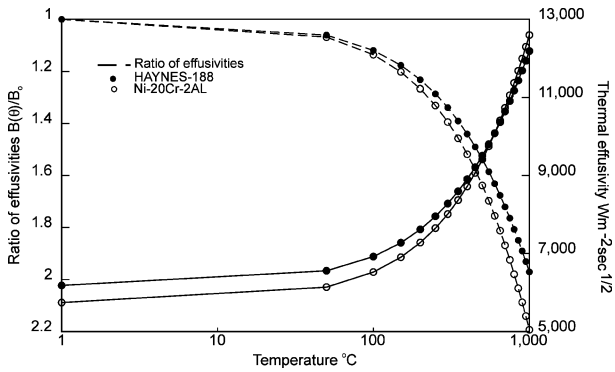

Figure 5. The variation in the thermal effusivity with temperature (right scale) and the ratio between the effusivity at the particular temperature and the effusivity at room temperature (left scale).

of the RRH in the presence of an oxide layer. Transition points pertaining to the Co-based alloy are marked by the letter T while those pertaining to the Ni-based alloy are identified by the letter S. Transition points that are located within the discrete points on the plot are reported as intervals. Thus, the graphically extracted transition temperatures for the Co-based alloy are 230 °C, 560 °C and 790 $< \theta <$ 825 °C, whereas those associated with the Ni-based alloy are 435 °C, 500 $< \theta <$ 525 °C, 600 $< \theta <$ 625 °C and 800 $< \theta <$ 830 °C. Those values are in good agreement with the experimentally determined temperatures (see *table III*).

Figure 5 entails two plots for each alloy: the variation in the thermal effusivity with temperature (right scale) and the ratio of the effusivity at the particular temperature to the effusivity at room temperature (left scale). Note that at a temperature corresponding to T1, the Haynes-188 exhibits a change in the slope of the effusivity. Moreover, the points T2, T3 and S1–S3 are located within a temperature interval (525 $< \theta <$ 850 °C) at which the effusivities of both alloys are approximately equal. Thus, the wear behavior of the studied alloys may be divided into three regions: initial wear reduction [0 °C–θ_{T1}, 0°C–θ_{S1}], secondary (local) transition [θ_{T1}–θ_{T2}, θ_{S2}–θ_{S3}], and primary wear transition [θ_{T2}–$\theta > \theta_{T3}$, θ_{S3}–$\theta > \theta_{S4}$].

Initial wear reduction is associated with a change in the sign of the RRH from a negative (indicating that

HDC $< Q_{gen}$) to a positive (indicating that HDC $> Q_{gen}$). This change corresponds to an initial growth period where the oxide attempts to overcome the energy barriers exerted by pressure, temperatures, and chemical composition of the alloys. The protective film starts discontinuous and as its thickness and area grow, partial separation between the rubbing materials will take place and a decrease in wear volume will follow. The zone of oxide formation is at the gas–oxide interface. The diffusion of oxygen in oxides is lower than that of the metal in oxides. Protective layer formation, therefore, requires the metal ions from the matrix to diffuse outward through the oxide layers. Since there is an abundance of oxygen at the surface, the diffusivity of the material in the oxides determines the growth rate. This means that the temperature (or synonymously, the available thermal energy) at the formation front and the length of the time through which this energy is available will control the distance the material atoms can travel. Thus, thermal energy that is in abundance in combination to longer times of energy availability will aid the growth of a protective oxide.

The secondary transition range for the Co-based alloy entails further reduction in wear volume. This is associated with a decrease in the available thermal energy (RRH is positive). The energy decrease is compensated by an increase in the intensity of frictional heat (i.e., concentration of thermal energy) within the contacting layer as indicated by the increase in F_1. Additionally, the effusivity of the alloy continues to increase with temperature. This implies an increase in the time interval through which heat is retained within the contacting layer. In contrast, through the same interval the Ni-based alloy exhibits an increase in the wear volume. Interestingly, at θ_{S2} and θ_{S3} the RRH is equal to zero. This indicates a balance between the HDC and the generated heat. Concurrently, heat intensity increases (note the considerable increase in F_1). The increase in F_1 is also accompanied with an increase in the effusivity, hence implying, again, an increased specific time of thermal energy availability. Therefore, the opposite wear behavior noted in this region may be attributed to nature of change in the function F_1 with temperature. The change in F_1 for both alloys promotes oxide growth through focusing the frictional heat within the true area of contact. However, the high intensification effect in the case of the Ni-based alloy will aid the growth of a thicker oxide film. The growth of that film will cause the effective conductivity of the film-substrate combination to drop (see equation (19)). The drop in the conductivity will tend to insulate the substrate. This will cause a considerable temperature difference between the film and the substrate. Now, since the oxide has a different coefficient of thermal expansion considerable stresses will develop at the boundary and wear debris will detach from the material. The detachment of wear debris will expose the underlying metal. The freshly exposed material being of higher effusivity and HDC than the oxide will admit a greater amount of heat. This, in turn, will be retained within the contacting layers for a longer period and an oxidative reaction will be sustained and the oxide layer will be repaired. The rate by which the oxide is repaired depends on the optimal combination of F_1 and effusivity (the determination of that combination remains a subject of ongoing research). It is worth noting that this self-repair characteristic was observed by Bill [21] for the Haynes-188 alloy.

Contrasting wear behaviors were also noted in the primary transition region. The increase in the HDC for the Co-based alloy is greater than the corresponding increase for the Ni-based alloy. This implies that a major portion of the heat conducted through the interface for the Ni-based alloy will be retained within the contact layer. The heat will be highly intensified within a smaller area due to the increase in F_1 (compare the increase in F_1 for both alloys). Interestingly, for this particular temperature range the effusivity of both alloys is equal. However, the ratio of the effusivity for the Ni-based alloy is higher than that for the Co-based alloy. This indicates a higher resistance to abrupt changes to the thermal state for the Ni-based alloy than that of the Co-based alloy. The combination of increased intensity and a higher resistance to thermal perturbations may change the oxidation kinetics for this temperature range. Again, this will promote the growth of a hard oxide film on a softer metallic substrate, an occurrence that will promote higher stresses that will cause the detachment of wear particles. Detachment of wear debris will introduce additional heat sources due to the rubbing of the debris with the surface. This causes a decrease in the HDC and a change in the slope of the RRH–temperature curve. Continuous rubbing of the debris will increase the coefficient of friction and will lead to higher release of friction heat. The debris, themselves, will react with the oxygen present at the surface. This will lead to a relative decrease in the amount of oxygen available for an oxidative reaction thereby, locally, slowing the growth of the protective layer. Due to the reduction in the effective conductivity, associated with the formation of the oxide, the RRH curve will deviate from the calculated values, probably following the schematic curves III. However, in the absence of complete thermal characterization of the oxides formed in the sliding of these particular alloys, exact calculations cannot be performed.

5. CONCLUDING REMARKS

This work suggests a connection between wear transition and the change in the heat transfer limit of a rubbing material. The nature of change in the thermal properties before and after the transition influences the thermal environment within the contacting layers. This controls the kinetics of oxide formation and thereby controls wear.

An important factor is the function F_1 which indicates the intensity of thermal energy available within the contacting layers. A high F_1 value and a high effusivity will promote the growth of a protective layer. The protective layer will affect the effective conductivity of the interface and may alter the thermal environment at the contact zone.

There is a pressing need for the thermal characterization of the oxides formed during sliding in order to quantify the effect of an oxide film on the HDC of a material. This will help to obtain an enhanced view of the thermal aspects of wear transition.

It is acknowledged that other parameters influence wear resistance at elevated temperatures. However, it is postulated that thermal energy release in rubbing may be crucial in providing an optimal heat environment for wear resistance. That is, depending on the ability of the rubbing pair to accommodate a sudden change in its thermal state, ambient conditions may be conducive for protective oxide formation and vice versa.

REFERENCES

[1] Bian S., Maj S., Borland D.W., The unlubricated sliding wear of steels, the contact conditions in the sliding zone, ASTM JTEVA 24 (1996) 12–19.

[2] Dayson A., Scuffing a review, Trib. Int. 8 (1975) 77–87, 117–122.

[3] Meng J., The investigation of steel seizure with disc machine, Friction and Wear of Machines 14 (1960) 222–237.

[4] Jeng H.H., True friction power intensity and scuffing in sliding contacts, ASME J. Trib. 120 (1998) 829–834.

[5] Blok H., Les temperatures des surfaces dans des condition de graissage sous pression extrême, in: 3ème Cong. Mondial Pétrole, 1937, pp. 471–486.

[6] Blok H., The postulate about the constancy of scoring temperatures, in: Ku P.M. (Ed.), NASA SP, Vol. 237, 1970, pp. 153–248.

[7] Wang N., The transformation of soft abrasive wear to hard abrasive wear under the effect of frictional heat, STLE Trans. 32 (1989) 85–90.

[8] Singh J., Alpas A.T., High-temperature wear and deformation processes in metal matrix composites, Metallurgical Materials Trans. A 27 (1996) 3135–3148.

[9] Zhang J., Alpas T.A., Transition between mild and severe wear in aluminium alloys, Acta Mater. 45 (1997) 513–528.

[10] Wilson S., Alpas A.T., Wear mechanism maps for metal matrix composites, WEAR 212 (1997) 41–49.

[11] Lim S.C., Ashby M.F., Wear mechanism maps, Overview no. 55, Acta Metall. 35 (1987) 1–24.

[12] Buckly D., Surface Effects in Adhesion, Friction, Wear and Lubrication, Tribology Series, Vol. 5, Elsevier, Amsterdam, 1981.

[13] Abdel-Aal H.A., The correlation between thermal property variation and high temperature wear transition of rubbing metals, WEAR 237 (2000) 145–151.

[14] Abdel-Aal H.A., On the influence of thermal properties on wear resistance of rubbing metals at elevated temperatures, ASME J. Trib. 122 (2000) 657–660.

[15] Özişik M., Necati, Boundary value problems of heat conduction, Dover, New York, 1989.

[16] Abdel-Aal H.A., A remark on the flash temperature theory, Int. Comm. Heat Mass Tran. 24 (1997) 241–250.

[17] Abdel-Aal H.A., On the thermal compatibility of metallic pairs in rubbing applications, Rev. Gén. Therm. 38 (1999) 27–41.

[18] Abdel-Aal H.A., A remark on the flash temperature theory, Int. Comm. Heat Mass Tran. 24 (2) (1998) 241–250.

[19] Abdel-Aal H.A., On the intrinsic thermal response of metallic pairs in dry sliding friction, Int. Comm. Heat Mass Tran. 26 (1999) 289–298.

[20] Abdel-Aal H.A., Error bounds of variable conductivity temperature estimates in frictionally heated contacts, Int. Comm. Heat Mass Tran. 25 (1998) 99–108.

[21] Bill R.C., Fretting of secondary-seal-candidate materials in air at temperatures to 816 °C, NASA TN D-7073, 1972.

[22] Bill R.C., Fretting of nickel–chromium–aluminium alloys at temperatures to 816 °C, NASA TN D-7570, 1974.

[23] Touloukian Y.S., Powell R.W., Ho C.Y., Niclaou M.C., Thermophysical Properties of Matter, Vol. 1, Plenum, New York, 1973.

[24] Marscher W.D., A critical evaluation of the flash-temperature concept, ASLE Preprint No. 81-AM-1D-3, 1981.